

TIME-DEPENDENT NON-STEADY-STATE DIFFUSIVITIES OF C6 PARAFFINS IN SILICALITE BY ZERO-LENGTH COLUMN METHOD*

Daniel SHAVIT^a, Patrick VOOGD^{b, **} and Herman W. KOUWENHOVEN^a

^a *Technisch Chemisches Labor, ETH-Zürich,
Universitätsstrasse 6, 8092 Zürich, Switzerland*

^b *Laboratory of Organic Chemistry, Delft University of Technology,
Julianalaan 136, 2628 BL Delft, The Netherlands*

Received September 13, 1991

Accepted October 14, 1991

Long-time diffusion experiments of n-hexane, 2-methylpentane and 2,3-dimethylbutane in silicalite according to the zero-length column method showed a significant decrease of the diffusion coefficients for longer times. A new and simple model of "uncoupled dual diffusion" is proposed to fit the experimental data. The calculated fast-diffusion coefficients as well as the calculated mean activation energies of diffusion of n-hexane and 2-methylpentane were almost equal and in reasonable agreement with literature data. A decrease of the adsorption partial pressure from 5.5 to 0.6 Torr did not have any influence on the fast-diffusion coefficient of n-hexane, which implies that the decrease of the diffusion coefficient in this range is not simply due to a non-linear isotherm. The proposed dual diffusion model may represent effects such as the presence of multiple energy states available for adsorbed molecules in the zeolite lattice, and/or diffusion anisotropy due to differences in the channel configurations in the three crystallographic directions.

Understanding intracrystalline diffusivities is important for the interpretation of reaction and adsorption selectivities. It has been shown repeatedly¹⁻³ that differences of several orders occur in reported diffusivities, depending to a large extent on definitions and usage of different formalisms. Terms, like "effective", "steady-state", "non-steady-state", "intrinsic", and "uptake"-diffusivities are all based on an assumed or implied mechanism.

Diffusivities are commonly corrected to intrinsic diffusivities for the concentration dependency due to the non-linearity of the isotherm applying Darken's equation. As a result both the intrinsic diffusivity and the activation energy for diffusion may differ significantly from the measured values⁴. Moreover, the intrinsic diffusivities may still be dependent on experimental concentrations (cf. methods sorbate uptake⁴, pulsed-field gradient NMR (ref.²), (PFG-NMR), single step frequency response⁵).

* Presented as a poster at the *International Symposium "Zeolite Chemistry and Catalysts"*, Prague, September 8-13, 1991.

** Present address: Lonza LDT Visp, 3930 Visp, Switzerland.

Non-steady-state methods (like zero-length column and sorbate uptake methods) are all based on a formalism of linear isothermic behaviour. Systems which are measured outside of the linear part of their isotherm, will not satisfactorily fit over the total time (= concentration) range.

In their recent work, Nowak et al.⁶ presented a molecular diffusion study on three-dimensional migration of short hydrocarbons in ZSM-5. The average of the computed steady-state diffusivities for methane and ethane ($D_{\text{tot}} = (D_x + D_y + D_z)/3$) were in satisfactory agreement with the results of PFG-NMR measurements.

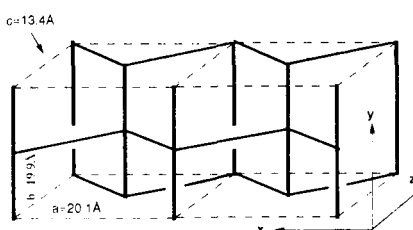
For methane as adsorbate in the MFI structure, a diffusion anisotropy ($D_x \neq D_y \neq D_z$) was simulated by a random walk model⁷. A molecular dynamics simulation of the butane diffusivity showed a similar diffusion anisotropy⁸. A direct determination⁹ of diffusion anisotropy of methane has become possible in PFG-NMR experiments with oriented H-ZSM-5 crystallites: The mean diffusivity in the direction of the two channel systems (straight and sinusoidal) was found to be about 5 times larger than the diffusivity in the third direction (Fig. 1).

If we assume, that at any one time, the total diffusion can be described as a superposition of different diffusion pathways, this would result in a time dependence of non-steady state diffusivities, even if the isotherms are linear: At the beginning of an experiment, one measures the fast diffusing pathway and the contribution of slow diffusion is nearly negligible. Upon depletion of the fast desorption pathway the situation may arise that the desorption rate is controlled by the slow desorbing path. A system characterized by a direction dependent mobility of the adsorbate, may accordingly show time-dependent non-steady-state diffusivity, even if the isotherm is linear.

In this paper we report long time desorption measurements (ZLC) using a new model to describe the behaviour of n-hexane, 2-methylpentane and 2,3-dimethylbutane in silicalite. The results obtained by the zero-length-column (ZLC) technique, which prevents mass and heat transfer limitations, will be compared with published data.

FIG. 1

Outline of channel network of ZSM-5 type zeolites over two adjacent unit cells. The straight and zig-zag channels are oriented along the y and x directions, respectively (1 Å = 0.1 nm)



THEORETICAL

In order to illustrate the concentration dependency of non-steady-state diffusivities, a zeolitic diffusion model, which was proposed by Hayne¹⁰ and extended by Garcia and Weisz³ will be briefly discussed.

Postulating a mobile phase, contributing to the stochastic movement, and a strongly adsorbed, immobilized phase, which is in equilibrium with the mobile one, the two Fick equations are written as:

$$\text{flux} = -D \frac{\delta C_m}{\delta x}, \quad (1)$$

$$D \frac{\delta^2 C_m}{\delta x^2} = \frac{\delta C_t}{\delta t}. \quad (2)$$

The symbols and indexes denote: D , diffusion coefficient; C , concentration in gaseous phase; index t , total amount of adsorbate; index m , mobile amount of adsorbate. Flux has units mol/m²s.

In summary, the assumption is made, that only the mobile phase (C_m) contributes to the process of diffusion. To describe the equilibrium between the mobile and immobilized phase, a linear isothermic relationship was proposed for both phases:

$$C_t = HC^\circ, \quad (3)$$

$$C_m = MC^\circ. \quad (4)$$

Combining Eqs (3) and (4) with Eqs (1) and (2) results in:

$$\text{flux} = -DM \frac{\delta C^\circ}{\delta x} = -D_{ss} \frac{\delta C^\circ}{\delta x}, \quad (5)$$

$$D \frac{M}{H} \frac{\delta^2 C^\circ}{\delta x^2} = \frac{\delta C^\circ}{\delta t} = D_{ns} \frac{\delta^2 C^\circ}{\delta x^2}. \quad (6)$$

D is intrinsic diffusivity, index ss means steady-state, index ns non-steady-state.

Non-steady-state measurements (uptake rate, ZLC, chromatographic method) are evaluated using Eq. (6) and yield the non-steady-state diffusivity D_{ns} , which is a function of M and H (Eq. (8)). On the other hand, steady-state determinations (catalytic reaction, quasi steady-state: differential uptake rate) are dealing with Eq. (5), resulting in steady-state diffusivities D_{ss} , which are a function of M only (Eq. (7)).

$$D_{ss} = MD \quad (7)$$

$$D_{ns} = \frac{M}{H} D \quad (8)$$

The important result is a non-equality of measured steady-state and non-steady-state diffusivities by a factor of the size of the Henry coefficient H . For measurements at low partial pressures ($p < 1$ kPa) the latter has usually a value between 100 and 10 000.

$$D_{ss} = D_{ns}H \quad (9)$$

Published PFG-NMR (steady-state) diffusivities are often several orders of magnitude higher than those measured by ZLC or gravimetric uptake rate (e.g. propane in silicalite at 334 K: PFG-NMR (ref.¹²): $3 \cdot 10^{-5}$ cm²/s; square wave⁵: $2 \cdot 5 \cdot 10^{-5}$ cm²/s; ZCL (ref.¹): $1 \cdot 2 \cdot 10^{-7}$ cm²/s).

By using a Arrhenius formalism in Eq. (9), Eq. (10) is obtained:

$$D_{ss}^\circ \exp\left(-\frac{E_{ss}}{RT}\right) = D_{ns}^\circ \exp\left(-\frac{E_{ns}}{RT}\right) H^\circ \exp\left(-\frac{\Delta H_{ads}^\circ}{RT}\right) \quad (10)$$

and therefore

$$D_{ss}^\circ = D_{ns}^\circ H^\circ, \quad (11)$$

$$E_{ss} = E_{ns} + \Delta H_{ads}^\circ. \quad (12)$$

In good agreement with literature data, activation energies E_{ss} of steady state measurements are predicted to be smaller (the standard adsorption enthalpy ΔH_{ads}° is negative) than the non-steady-state activation energies E_{ns} (e.g. propane at 334 K in silicalite: PFG-NMR (ref.¹²): 7.5 kJ/mol; square wave⁵: 6.7 kJ/mol; ZLC (ref.¹): 12.5 kJ/mol). As shown by Voogd and van Bekkum⁴, for temperatures around 75°C, the isotherms of n-hexane and 3-methylpentane in silicalite are linear for $p/p^\circ < 2 \cdot 10^{-4}$. By using a Langmuir or a Vollmer isothermic behaviour (Fig. 2), the equation of Darken:

$$D_{app} = D \frac{d \ln P}{d \ln C} \quad (13)$$

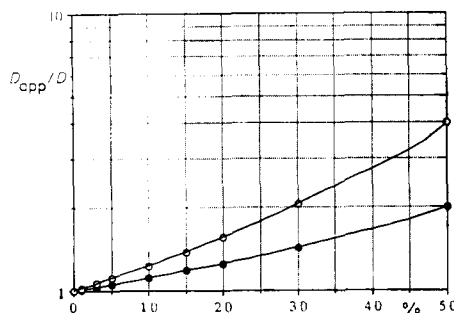


FIG. 2

Effect of the relative saturation of the zeolite (%) on the calculated D_{app}/D . ● Langmuir isotherm, ○ Vollmer isotherm

becomes¹³:

$$D_{app} = \frac{D}{(1 - C/C_s)^n}. \quad (14)$$

For the Langmuir isotherm: $n = 1$, Vollmer isotherm: $n = 2$, D means intrinsic diffusivity and D_{app} is apparent diffusivity.

Systems, which are not behaving linear in their isotherms, will provoke a time dependency of fitted non-steady-state diffusivities (ZLC, sorbate uptake), which are always based on linear isotherm relationships. If no time dependency of the fitted (and mean) non-steady-state diffusivity can be found, there is no measurable deviation from the linear isotherm behaviour, and therefore no reason for any non-linearity correction.

Zero Length Column Method

As already described elsewhere¹⁴⁻¹⁶, it is assumed that at the applied high carrier gas flow rate the concentration of adsorbate at the crystal surface during desorption is nearly zero and that heat transfer from the zeolite to the gas phase is fast. The desorption is accordingly fully controlled by intracrystalline diffusion. In this case, the solution for spherical crystals is:

$$\frac{C}{C^\circ} = 2L \sum_{i=1}^{\infty} \frac{\exp(-\beta_i^2 Dt/R^2)}{\beta_i^2 + L(L-1)} \quad (15)$$

β_i is given by the positive roots of:

$$\beta_i \cot \beta_i + L - 1 = 0 \quad (16)$$

with L equal to:

$$L = \frac{\varepsilon v R^2}{3(1 - \varepsilon) HDZ} = \frac{V' R^2}{3V_z HD}. \quad (17)$$

The symbols denote: C , sorbate concentration in the gas phase at time t ; C° , concentration before desorption ($t = 0$); D , non-steady-state diffusivity; t , time; R , characteristic diffusion length; ε , voidage of zeolite bed; v , interstitial gas velocity; H , Henry coefficient (assumed linear isotherm); Z , depth of zeolite bed; V' , gas flow velocity; V_z , crystal volume.

It was calculated, that for $0.0001 < D/R^2 < 0.1$ and $1 < L < 1000$ and $t < 10$ s, the use of 15 terms (β_i) for the simulation of $\ln(C/C^\circ)$, produces less than 0.5% error.

Eq. (15), which describes the measurable concentration in the gas phase as a function of time, diffusivity and L -value, stands for a mono diffusion model of linear isothermic behaviour. Any non linearity of the isotherm or parallel diffusion (due to direction dependent mobility) should be discovered as a significant, systematic deviation of the fitted curve for longer times. For the case that this time dependent deviation of the ideal diffusion behaviour occurs, we propose a model of two uncoupled diffusion pathways. If the desorption of adsorbate via a fast-diffusion path is assumed to have minor influence on the desorption of a slow-diffusion path and vice versa, then the solution is a simple summation of both desorptions:

$$\frac{C_{\text{tot}}}{C^\circ} = \frac{C_f + C_s}{C^\circ} = 2L_f \sum_{i=1}^{\infty} \frac{\exp(-\beta_{f,i}^2 D_f t / R^2)}{\beta_{f,i}^2 + L_f(L_f - 1)} + 2L_s \sum_{i=1}^{\infty} \frac{\exp(-\beta_{s,i}^2 D_s t / R^2)}{\beta_{s,i}^2 + L_s(L_s - 1)}. \quad (18)$$

Indexes: tot, measured total signal; f, from fast desorbing path; s, from slow desorbing path. For longer times, the solution becomes:

$$\frac{C_{\text{tot}}}{C^\circ} = \frac{C_f + C_s}{C^\circ} = 2L_f \frac{\exp(-\beta_{f,1}^2 D_f t / R^2)}{\beta_{f,1}^2 + L_f(L_f - 1)} + 2L_s \frac{\exp(-\beta_{s,1}^2 D_s t / R^2)}{\beta_{s,1}^2 + L_s(L_s - 1)}. \quad (19)$$

According to Eq. (19) a plot of $\ln(C_{\text{tot}}/C^\circ)$ versus t will show two linear regions connected by a transitional region. The first short-time linear region is mainly controlled by the first term (D_f) of the equation, while the second one is negligible. For very long times ($t \gg 0$), the second term (D_s) will be dominant while the first one is negligible and Eq. (19) becomes:

$$\ln\left(\frac{C_{\text{tot}}}{C^\circ}\right) = \ln\left(\frac{2L_s}{\beta_{s,1}^2 + L_s(L_s - 1)}\right) - \frac{\beta_{s,1}^2 D_s t}{R^2}. \quad (20)$$

Thus, a model of two uncoupled diffusion coefficients will show two characteristic linear regions differing in slope, both being directly proportional to the corresponding diffusion coefficients.

Using (15) and the fitted values D and L , the Henry coefficients H are calculated:

$$H = \frac{V' R^2}{3V_z L D}, \quad (21)$$

$$V_z = \frac{m}{\varrho_z}. \quad (22)$$

The apparent density $\varrho_z = 1.15 \text{ g/cm}^3$ of silicalite is calculated from the framework density¹⁷ of 17.9 tetrahedra (SiO_2) per 1000 \AA^3 .

EXPERIMENTAL

Zero Length Column Apparatus

The zero-length column (also described in ref.¹⁰ and ref.¹⁴), consisted of a Swagelock stainless steel tube connector containing 1–3 mg of zeolite pressed between small quartz wool plugs. The applied flow rate of 11.5 ml/min (gas space velocity > 1900 min⁻¹) was high enough to result in a negligible film resistance. The sample was activated in situ by heating 2 h at 700 K. All data were corrected for any extracrystalline effects due to the equipment used, measured using an empty reactor. The measured signal is defined by:

$$\ln \left(\frac{C}{C^\circ} \right) = \ln \left(\frac{I - I^\infty}{I^\circ - I^\infty} \right), \quad (23)$$

where I is signal at time t , I^∞ signal at $t = 2500$ s (zero line); $t \approx \infty$, I^0 signal at $t = 0$. Corrected relative signal is

$$\ln \left(\frac{C_{\text{corr}}}{C^\circ} \right) = \ln \left(\frac{C}{C^\circ} - \frac{C_b}{C^\circ} \right), \quad (24)$$

where C_{corr} is corrected signal, C_b correction.

The standard deviation of $\ln (C_{\text{corr}}/C^\circ)$ was found in repeated measurements to be less than 10% for all times between 15 and 400 s. Fits of C_{corr}/C° versus t (Eq. (16)) result in values of D_f , L_f , D_s and L_s . Errors in the diffusivities and the values of L were estimated to be 20 and 30%, respectively.

Silicalite

Silicalite was prepared according to the method of Kessler and Buth¹⁸ by mixing 26 g silica sol (Ludox AS40, Dupont) with 12 g tetrapropylammonium bromide (TPABr, Fluka, >99.5%) and 6.5 g ammonium fluoride (Fluka >99.5%) in 17 ml of demineralized water. The starting mixture with molar ratios of $(\text{NH}_4)_2\text{O} : \text{SiO}_2 : 19 \text{ H}_2\text{O} : 2 \text{ HF} : 0.26 \text{ TPABr}$ was heated in a polypropylene bottle at 100°C for 6 days (no stirring). After filtration, the product was washed with demineralized water, dried at 100°C and calcined at 550°C for 1 h. The sample was characterized by XRD (Rigaku, CuK α), ammonia-TPD, FTIR, SEM and BET (Mikromeritics Asap 2000).

RESULTS AND DISCUSSION

Properties of the silicalite used in our experiments are collected in Table I. It appears, that the material is highly crystalline and consist of 17 × 17 × 48 μm crystals twinned at an angle of 90°. Ammonia temperature programmed desorption (NH₃-TPD) showed that the material did not contain strong acid sites.

As shown in Fig. 3 the $\ln (C/C^\circ)$ vs time curve consists of a transitional part and two linear parts. The latter differ in slope and consequently in diffusion coefficient, the measured diffusion coefficients becoming significantly smaller after a measuring time of 50–100 s. Values of $\ln (C/C^\circ)$ vs time calculated according the current

"monodiffusion" model (Eqs (15)–(17)), may be calculated considering either the initial slope of the $\ln(C/C^0)$ vs time curve or its final slope. In both cases the calculated and measured $\ln(C/C^0)$ vs time curves will only fit for the period considered in the calculation of D .

Alternatively a concentration dependent diffusion coefficient, based on a non-linear isotherm, might be applied for the calculation of the $\ln(C/C^0)$ vs time curve. We

TABLE I
Properties of the used silicalite Z882

Method	Property
XRD/FTIR	Structure: MFI
BET (N_2)	$V_{\text{micro}} = 0.136 \text{ cm}^3/\text{g}$
SEM	Area: $347 \text{ m}^2/\text{g}$
Crystal size distribution	Size: $17 \times 17 \times 43 \mu\text{m}$
$\text{NH}_3\text{-TPD}$	90° twinning used $R: 8.5 \mu\text{m}$ narrow no Brønsted acid sites

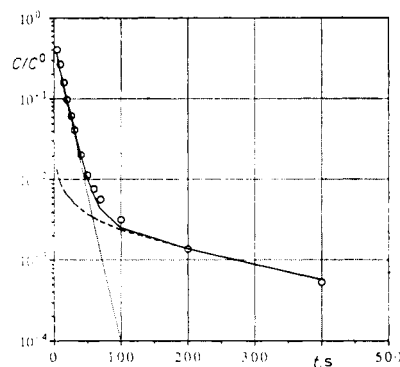


FIG. 3

The diffusion of 2-methylpentane at 160°C: Comparison of experimental curve with that calculated using the dual diffusion model. ○ Measured signal, C_f/C^0 , - - - C_s/C^0 , — $(C_f + C_s)/C^0$

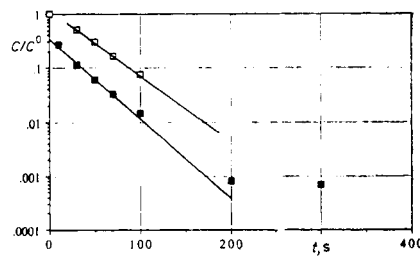


FIG. 4

Effect of the adsorption partial pressure of the adsorbate on the diffusivity of n-hexane at 140°C. ■ Pressure 5.5 Torr, $D_f = 2.9 \text{ e} - 9 \text{ cm}^2/\text{s}$; □ pressure 0.6 Torr, $D_f = 28 \text{ e} - 9 \text{ cm}^2/\text{s}$

found, that lowering the partial pressure during n-hexane adsorption at 140°C from 5.5 to 0.6 Torr (1 Torr = 133 Pa) had no effect on the value of the initial diffusivity (Fig. 4), which implies, that the initial diffusivity in this range is not concentration dependent.

A calculation of the $\ln(C/C^0)$ vs time curve using two independent coefficients D_f and D_s , describing both the two linear and the transition parts of $\ln(C/C^0)$ vs time curve, results in a close fit of measured and calculated curves (Fig. 3).

A comparison of the "fast-diffusion" coefficients D_f found here for n-hexane, 2-methylpentane and 2,3-dimethylbutane with D values reported in the literature is presented in Fig. 5. At higher temperatures, a reasonable agreement with published data is found for n-hexane. The data for 2-methylpentane extrapolate to the reported point at 343 K. For 2,3-dimethylbutane D_f values found here are about 10 times higher than earlier data, which were obtained by the gravimetric uptake rate method.

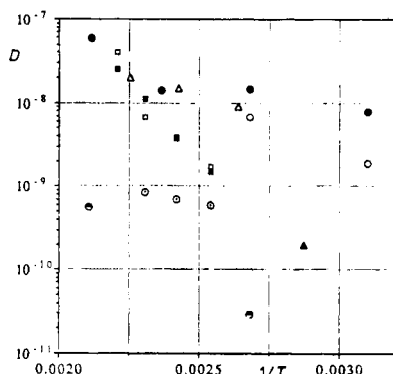


FIG. 5

Arrhenius plot of the diffusion coefficients ($\text{cm}^2 \text{ s}^{-1}$) of the fast desorbing path (D_f) of \square n-hexane, \blacksquare 2-methylpentane and \circ 2,3-dimethylbutane in silicate with literature data: \circ n-hexane diffusivity on silicalite measured by ZLC (ref.¹⁴); \bullet n-hexane diffusivity on silicalite containing 90° intergrowths (ZLC (ref.¹⁴)); \triangle n-hexane diffusivity on silicalite measured by Single Step FR (ref.⁵); \blacktriangle 3-methylpentane diffusivity on ZSM-5 measured by the Thiele method²⁰; \bullet 2,3-dimethylbutane diffusivity on silicalite measured by gravimetric uptake²¹

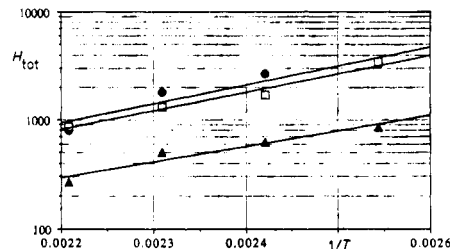


FIG. 6

Arrhenius plot of the calculated overall Henry coefficients $H_{\text{tot}} = H_f + H_s$: \bullet n-hexane; \square 2-methylpentane; \blacktriangle 2,3-dimethylbutane

TABLE II
Calculated diffusion coefficients D_f and D_s as a function of adsorbate and temperature based on ZLC measurements

Adsorbate	$T, ^\circ\text{C}$	$D_f \cdot 10^9$ cm^2/s	L_f	$D_s \cdot 10^9$ cm^2/s	L_s
n-hexane	120	1.7	10.5	0.22	220
2-methylpentane	120	1.5	9.0	0.21	680
2,3-dimethylbutane		0.59	120	0.15	183
n-hexane	140	2.8	5.2	0.48	105
2-methylpentane	140	3.8	7.5	0.41	470
2,3-dimethylbutane		0.70	160	0.15	239
n-hexane	160	6.7	3.8	0.49	820
2-methylpentane	160	11	3.3	0.51	600
2,3-dimethylbutane		0.86	120	0.16	315
n-hexane	180	40	0.53	—	1100
2-methylpentane	180	25	2.6	0.76	250
2,3-dimethylbutane		— ^a	— ^a	0.2	318

^a No fast diffusion path was observable.

TABLE III
Activation energies of measured non-steady-state diffusivities D_f and D_s and calculated steady-state diffusivities $D_{ss} = D_{ns} + \Delta H_{ads}^\circ$

Activation energy	n-Hexane	2-Methylpentane	2,3-Dimethylbutane
$E_f, \text{kJ/mol}$	74 ± 8	71 ± 8	13 ± 8
$E_s, \text{kJ/mol}$	29 ± 5	30 ± 5	7 ± 5
$E_m = (E_f + E_s)/2$	51 ± 5	51 ± 5	10 ± 5
$-\Delta H_{ads}^\circ, \text{kJ/mol}$	33 ± 3	33 ± 3	27 ± 3
$E_{ss}, \text{kJ/mol}$	18 ± 6	18 ± 6	—17 ± 6
Lit. data: $E_{ss}, \text{kJ/mol}$	ref. ⁵ : 17		
Lit. data: $E_{ns}, \text{kJ/mol}$	ref. ¹⁴ : 14—48 ^a ref. ¹⁴ : 25 ^b	ref. ²⁰ : 48	ref. ²¹ : 42 ^c

^a Calculated for $112 < T < 200^\circ\text{C}$, points of b in Fig. 4; ^b only two measurements, points of a in Fig. 4; ^c only two measurements.

Overall Henry coefficients (H_{tot}) were calculated according to Eqs (23) and (24). Using the data from Table II, a plot of the values is presented in Fig. 6. The resulting values of $-\Delta H_{\text{ads}}^{\circ}$ for each of the adsorbates, which are presented in Table III, are found to be around 30 kJ/mol. Recently Pal et al.¹⁹ reported a value of 37.8 kJ/mol for $\Delta H_{\text{ads}}^{\circ}$ of n-hexane on ZSM-5, which is close to our value 33.4 kJ/mol measured on the much less polar silicalite.

The calculated activation energies for non-steady-state fast and slow diffusion E_f and E_s are collected in Table III. E_f values for n-hexane and 2-methylpentane found here are some 50% higher than the values of E_{ns} based on mono diffusion models, published earlier. The mean activation energies E_m are however in good agreement with earlier values.

The steady-state activation energy, E_{ss} , for n-hexane calculated from the standard enthalpy of adsorption $\Delta H_{\text{ads}}^{\circ}$ following Eq. (12) is in agreement with the values of E_{ss} measured in single-step frequency response experiments.

The proposed dual diffusion model may represent effects such as the presence of multiple energy states available for adsorbed molecules in the zeolite lattice or diffusion anisotropy due to differences in the channel configurations in the three crystallographic directions or a combination of these effects.

REFERENCES

1. Kärger J., Ruthven D. M.: *Zeolites* **9**, 267 (1989).
2. Kärger J., Ruthven D. M.: *J. Chem. Soc., Faraday Trans. 1* **77**, 1485 (1981).
3. Garcia S. F., Weisz P.: *J. Catal.* **121**, 194 (1990).
4. Voogd P., van Bekkum H.: *Stud. Surf. Sci. Catal.* **46**, 519 (1989).
5. Begin N. V. D., Rees L. V. C., Caro J., Bülow M.: *Zeolites* **9**, 287 (1989).
6. Nowak A. K., Post M. F. M., den Ouden J. J., Pickett S. D., Smit B., Cheetham A. K., Tomas J. M.: *J. Phys. Chem.* **95**, 848 (1991).
7. Kärger J.: *J. Phys. Chem.* **95**, 5558 (1991).
8. Goodbody S. J., Watanabe K., MacGowan D., Walton J. P. R. B., Quirke N.: *J. Chem. Soc., Faraday Trans.* **87**, 1951 (1991).
9. Hong U., Kärger J., Kramer R., Pfeifer H., Müller U., Unger K. K., Lück H. B.: *Zeolites*, submitted.
10. Haynes H. W.: *J. Catal. Rev. Sci. Eng.* **30**, 363 (1988).
11. Atkins P. W.: *Physical Chemistry*, 2nd ed., p. 907. Oxford University Press, Oxford 1982.
12. Caro J., Bülow M., Schirmer W., Kärger J., Heink W., Pfeifer H.: *J. Chem. Soc., Faraday Trans. 1* **81**, 2541 (1985).
13. Garg D. R., Ruthven D. M.: *Chem. Eng. Sci.* **27**, 417 (1972).
14. Voogd P., van Bekkum H., Shavit D. H., Kouwenhoven H. W.: *J. Chem. Soc., Faraday Trans.*, submitted.
15. Eic M. L., Ruthven D. M.: *Zeolites, Facts, Figures, Future*, p. 897. Elsevier, Amsterdam 1989.
16. Eic M. L., Ruthven D. M.: *Zeolites* **8**, 40 (1988).

17. Meier W. M., Olson D. H.: *Atlas of Zeolite Structure Types*, 2nd. Butterworths, Cambridge 1987.
18. Guth J. L., Kessler H., Wey R.: *Developments in Zeolite Science and Technology, Proc. 7th. Int. Conf. on Zeolites*, p. 121. Elsevier, Amsterdam 1986.
19. Pal T. K., Majumder A., Raha T. K., Fetting F.: *Chem. Eng. Technol.* 13, 2948 (1990).
20. Voogd P., van Bekkum H.: *Appl. Catal.* 59, 311 (1990).
21. Voogd P., van Bekkum H.: *Ind. Eng. Chem. Res.*, in press.